THE JOURNAL OF BIOLOGICAL CHEMISTRY VOL. 285, NO. 49, pp. 38415–38427, December 3, 2010

Morphine Modulation of Thrombospondin Levels in Astrocytes and Its Implications for Neurite Outgrowth and Synapse Formation*[S]

Received for publication, February 2, 2010, and in revised form, September 28, 2010 Published, JBC Papers in Press, October 2, 2010, DOI 10.1074/jbc.M110.109827

Hiroko Ikeda[‡§1], Mayumi Miyatake[‡1], Noriaki Koshikawa[§], Kuniyasu Ochiai[¶], Kiyoshi Yamada[¶], Alexi Kiss[‡], Maureen J. Donlin[‡‖], W. Michael Panneton[**], James D. Churchill[‡‡], Michael Green[‖], Akbar M. Siddiqui[‖], Andrew L. Leinweber[‡], Nicholas R. Crews[‡], Lubov A. Ezerskiy[‡], Victoria R. Rendell[‡], Mariana M. Belcheva[‡], and Carmine J. Coscia[‡2]

From the [‡]E. A. Doisy Department of Biochemistry and Molecular Biology, [‖]Molecular Microbiology and Immunology, [**]Pharmacological and Physiological Sciences, and [‡‡]Psychology, St. Louis University, St. Louis, Missouri 63104 and the Departments of [§]Pharmacology and [¶]Microbiology, Nihon University School of Dentistry, Tokyo 101-8310, Japan

Opioid receptor signaling via EGF receptor (EGFR) transactivation and ERK/MAPK phosphorylation initiates diverse cellular responses that are cell type-dependent. In astrocytes, multiple μ opioid receptor-mediated mechanisms of ERK activation exist that are temporally distinctive and feature different outcomes. Upon discovering that chronic opiate treatment of rats down-regulates thrombospondin 1 (TSP1) expression in the nucleus accumbens and cortex, we investigated the mechanism of action of this modulation in astrocytes. TSP1 is synthesized in astrocytes and is released into the extracellular matrix where it is known to play a role in synapse formation and neurite outgrowth. Acute morphine (hours) reduced TSP1 levels in astrocytes. Chronic (days) opioids repressed TSP1 gene expression and reduced its protein levels by μ opioid receptor and ERK-dependent mechanisms in astrocytes. Morphine also depleted TSP1 levels stimulated by TGFβ1 and abolished ERK activation induced by this factor. Chronic morphine treatment of astrocyte-neuron co-cultures reduced neurite outgrowth and synapse formation. Therefore, inhibitory actions of morphine were detected after both acute and chronic treatments. An acute mechanism of morphine signaling to ERK that entails depletion of TSP1 levels was suggested by inhibition of morphine activation of ERK by a function-blocking TSP1 antibody. This raises the novel possibility that acute morphine uses TSP1 as a source of EGF-like ligands to activate EGFR. Chronic morphine inhibition of TSP1 is reminiscent of the negative effect of μ opioids on EGFR-induced astrocyte proliferation via a phospho-ERK feedback inhibition mechanism. Both of these variations of classical EGFR transactivation may enable opiates to diminish neurite outgrowth and synapse formation.

Astrocytes are the source of a diverse group of molecules that are required for synapse formation, function, and maintenance in neurons (1–7). Thrombospondin (TSP)[3] is a member of the astrocyte-derived intercellular signaling components that have been implicated in synaptogenesis and other neuronal glial interactions of the developing brain (8–17). In addition, synaptic plasticity and other neuroadaptations involving astrocyte neuron interactions are thought to play a role in reward learning and addiction (18). Some chronic morphine-responsive genes (Homer1, PSD-95, and synaptotagmin1) may subserve the long lived neuronal and behavioral plasticity observed in regions of the mesolimbic reward system, and they are involved in synaptogenesis (19–26).

TSPs are multidomain, multimeric glycoproteins that are secreted into the extracellular matrix of many cells and serve as bridging molecules in cell-cell interactions (27, 28). First discovered in platelet α-granules and secreted upon platelet activation, the superfamily of TSPs modulate varied functions of cell signaling and cell adhesion in a broad array of cell types. The five TSP genes are expressed in the CNS and peripheral nervous system where they play important roles in neural development. TSP1 promotes neurite formation and adhesion in neurons (29–32). Recently, a major breakthrough in astrocyte-neuron interactions occurred when TSP1/2 were shown to be important secretory astrocytic proteins that promote synapse formation in the developing brain (5, 10, 33, 34). Both *in vitro* and *in vivo* evidence have been presented. Similarly, TSP1 released by pluripotent bone marrow stromal cells promotes retinal ganglion cell survival and neurite outgrowth (35). Several independent research groups have reported that TGFβ increases TSP1 expression and/or protein levels in astrocytes as shown by immunoblotting, qRT-PCR, and/or *in situ* hybridization. In the initial report, TGFβ induced TSP1 in rat type 1 astrocytes as shown by counting silver grains/cell after *in situ* hybridization (36). In other studies on primary human astro-

* This work was supported, in whole or in part, by National Institutes of Health Grant DA-005412 (to C. J. C.). This work was also supported by individual research grant from Nihon University and a grant for promotion of multidisciplinary research projects from the Ministry of Education, Culture, Sports, Science and Technology (to H. I.).

[S] The on-line version of this article (available at http://www.jbc.org) contains a supplemental figure.

[1] Both authors contributed equally to this work.

[2] To whom correspondence should be addressed: Dept. of Biochemistry and Molecular Biology, St. Louis University School of Medicine, 1100 S. Grand Blvd., St. Louis, MO 63104. Tel.: 314-977-9254; Fax: 314-977-9205; E-mail: cosciacc@slu.edu.

[3] The abbreviations used are: TSP, thrombospondin; Ab, antibody; CaM, calmodulin; CTAP, D-Phe-Cys-Trp-Arg-Thr-Pen-Thr-NH_2; DAMGO, [D-Ala^2,mePhe^4,Gly-ol^5]enkephalin; EGFR, EGF receptor; G protein, GTP-binding regulatory protein; KOR, κ opioid receptor; MOR, μ opioid receptor; nor-BNI, norbinaltorphimine; qRT, quantitative RT; s.c., subcutaneous; MMP, matrix metalloproteinase.

cytes, TGFβ induced TSP1 expression as measured by the more quantitative methods of Western and Northern blotting and qRT-PCR (37, 38). TGFβ1and TGFβ2 stimulate TSP1 expression in epithelial cells and fibroblasts via EGFR transactivation and ERK and p38 MAPKs (39–41).

Astrocytes express many of the same G protein-coupled receptors, growth factors, and cytokine signaling systems found in neurons and other cells (42). These signaling molecules are involved in many novel functions of astrocytes, including communication with neurons during development and throughout adulthood. However, the mechanisms involved in this dynamic partnership with neurons are not well characterized. The targets of opiate drugs of abuse are opioid receptors, G protein-coupled receptors that are found in astrocytes and are capable of modulating their proliferation *in vitro* and *in vivo* (43–52). Using an astrocytoma model system, C6 glioma cells, and immortalized type 1 astrocytes, we implicated phosphatidylinositol turnover, discrete PKC isoforms, different secondary messengers, and transactivation of EGFR as well as FGF receptor in μ and κ opioid receptor (MOR and KOR) activation of ERK (53–57). Recently, we found that KOR agonists *stimulate* proliferation of immortalized and primary astrocytes via both rapid pertussis toxin-sensitive Gβγ- and sustained βarrestin2-dependent ERK pathways (58). *Acute* morphine and DAMGO activate ERK via G protein, calmodulin (CaM), and βarrestin2-dependent mechanisms. However, *chronic* treatment with these MOR agonists *inhibits* EGFR-stimulated ERK activation and proliferation of primary astrocytes (59). The G protein and β-arrestin2-dependent pathways were shown to be involved in the inhibition of astrocyte proliferation, but CaM signaling was not. Chronic morphine has been shown to modulate synaptic plasticity genes, a cellular response in addiction (20). Therefore, we decided to explore the possibility that it affects TSP1 expression in astrocytes.

Here, we show that acute (hours) morphine inhibits TSP1 protein levels in astrocytes. Moreover, chronic treatment (days) with opiates inhibits TSP1 gene expression *in vivo* and *in vitro*. Morphine diminishes cellular and media TSP1 protein levels in serum-deprived astrocytes via MOR and ERK. Both basal and TGFβ1-induced TSP1 is attenuated by morphine. Finally, chronic morphine treatment of astrocyte neuron co-cultures reduces neurite outgrowth and synapse formation.

EXPERIMENTAL PROCEDURES

Reagents—Chemicals and Abs were purchased from Sigma with the following exceptions: DAMGO, morphine sulfate, D-Phe-Cys-Trp-Arg-Thr-Pen-Thr-NH_2 (CTAP), norbinaltorphimine (nor-BNI), and buprenorphine from NIDA Drug Supply (Research Triangle Park, NC) or Daiichi Sankyo (Tokyo, Japan); human platelet-derived TSP1 from Hematologic Technologies (Essex Junction, VT); TGFβ from Austral Biologicals (San Ramon, CA); EGF, anti-TSP1 Ab, and U0126 from Calbiochem; trypsin/EDTA solution from Invitrogen; DMEM and fetal bovine serum (FBS) from ATCC (Manassas, VA); papain from Worthington; minimum Eagle's medium, N2 + B27 supplements, Alexa Fluor-labeled secondary Abs, and horse serum from Invitrogen; anti-phospho-ERK1/2 (directed against phospho-Thr-202/Tyr-204) Ab from Cell Signaling Technology (Beverly, MA); anti-glial fibrillary acidic protein Ab from Immuno Star, Inc. (Hudson, WI, catalogue no. 22522); anti-ERK Abs from Santa Cruz Biotechnology (Santa Cruz, CA); rabbit anti-synaptotagmin Ab from Synaptic Systems (Goettingen, Germany); mouse anti-PSD-95 Ab from BD Biosciences; chicken anti-MAP2 Ab from Covance (Emeryville, CA); anti-TSP1 Ab C6.7 (azide-free function-blocking antibody) and Ab-11 (immunoblotting) from LabVision (Fremont, CA); aminomethylcoumarin acetate-conjugated anti-chicken IgY from Jackson ImmunoResearch; and VECTASHIELD Mounting Medium from Vector Laboratories, Inc. (Burlingame, CA).

Immortalized Rat Type-1 Cortical Astrocyte Cultures—Rat cortical astrocytes (CTX TNA2; American Type Culture Collection) were established from cultures of primary type 1 astrocytes from 1-day-old rat brain frontal cortex. The cultures were originally transfected with a DNA construct containing the oncogenic early region of simian virus 40 under the transcriptional control of human glial fibrillary acidic protein promoter (60). The cells have the phenotypic characteristics of type 1 astrocytes. This cell line was maintained in DMEM + 10% FBS at 37 °C in a humidified atmosphere of 95% air, 5% CO_2 for up to 5–35 passages. Later passage cells (for the most part, 10–20) were transfected with MOR1 in our experiments as we found that they did not contain endogenous MOR or KOR by Western blotting (61). Therefore, in experiments with transiently transfected immortalized astrocytes, we observed an interaction of morphine with transfected MOR1. The amounts of MOR1 in transfected immortalized astrocytes are higher than levels of endogenous MOR in primary astrocytes in Western blots. Nevertheless, in parallel experiments with MOR1-transfected immortalized astrocytes and untransfected primary astrocytes, similar opioid signaling responses were observed in most cases (56–59). This supports the notion that the extent of MOR1 overexpression in immortalized astrocytes does not exceed the physiological range. Agonists, antagonists, or inhibitors were delivered in serum-free media.

Primary Astrocyte Cultures—Astrocytic cultures were prepared by modification of a method described previously (62). Postnatal day 1 Sprague-Dawley rat pups were euthanized, and their cortical regions were dissected, minced, suspended in 2.5 ml of ice-cold PBS, and trypsinized by incubation with an equal volume of 0.05% trypsin/EDTA solution at 37 °C for 15 min. The tissue was pelleted (1000 × *g* for 10 min), resuspended in 5 ml of DMEM containing 5% FBS and 5% horse serum, triturated, and plated onto poly-L-lysine (M_r 30,000–70,000)-coated tissue culture flasks as indicated. After 7 days in culture, the poly-L-lysine-coated flasks were shaken for at least 2 h, after which the unattached cells were removed and fresh culture medium was added (DMEM, 5% FBS + 5% horse serum). For ERK1/2 assay, growth medium was replaced with DMEM without serum 24 h prior to ligand treatment. Of the total number of cells in primary cultures, 90% were glial fibrillary acidic protein-positive and <1% were TuJ1 (neuronal marker)-positive (58).

Neuronal Cultures from Embryonic Rat Hippocampi—We adopted the Banker procedure modified by Laezza *et al.* (63). Briefly, a pregnant rat (E18–E19) was euthanized, and fetuses were removed. Fetal brains were then dissected out, and hippocampi were collected in calcium- and magnesium-free

Hanks' balanced salt solution. Tissue was then treated with freshly prepared papain (20 units/ml) solution as follows: Hanks' balanced salt solution, 0.2 mg/ml cysteine, 50 mM EDTA, and 100 mM $CaCl_2$. Cells were dissociated by pipetting, counted, and plated on poly-L-lysine-treated glass coverslips in redefined and modified neuronal plating media. Neurons were allowed to attach for 4–5 h by incubation at 37 °C and then co-cultured with astrocytes.

Co-cultures of Primary Astrocytes and Neurons—Primary astrocytes, prepared as described above but grown in minimum Eagle's medium containing 0.6% glucose 10% horse serum and antibiotics, were plated on poly-L-lysine-precoated cell culture inserts (BD Biosciences). A half-day before co-culturing, media in astrocytes were changed with neuronal maintenance media as follows: serum-free minimum Eagle's medium with N2 and B27 supplements, 1 mM pyruvate, 0.1% ovalbumin, and 20% glucose. Coverslips with attached neurons were transferred to plates containing astrocyte inserts. After 2–3 days, Ara-C was added to reduce microglial proliferation. The cultures were treated with 1 μM morphine on a daily basis for 8–9 days, and the ligand was added to the media in the inserts, where astrocytes were grown.

Transient Transfection—Immortalized astrocytes were transfected with rat MOR1 cDNA (in pCMV-neo expression vector) using FuGENE 6 transfection reagent (Roche Applied Science) following the manufacturer's instructions and using 1 μg of cDNA and 3 μl of transfection reagent. After 24 h of incubation, drug treatments were begun with serum-deprived media as vehicle. In some cases, cultures were co-transfected with pcDNA3 (for mock transfections), dominant negative MEK in pcDNA3 and rat MOR1 cDNA (pCMV-neo expression vector) using FuGENE 6 as described above.

In Vivo Drug Treatment for DNA Microarray Analyses—Fischer 344/Brown Norway F1 inbred male rats were administered either vehicle or buprenorphine (2.5 mg/kg/day) intraperitoneally for 14 days and the animals allowed to withdraw spontaneously for 9 days. Rats were anesthetized with CO_2 until comatose and sacrificed by cervical decapitation. Heads were transferred to a stereotaxic device (Kopf Instruments), and their dorsal cranium was removed. A 1.5-mm slice of brain was made stereotaxically through levels of the nucleus accumbens (antero-posterior levels between 0.7–2.2 mm anterior to bregma), and the whole brain was carefully extirpated. The slice was dissected free from the forebrain, placed on a glass slide, and frozen on dry ice. The nucleus accumbens surrounds the anterior commissure, which is grossly visible. A 1.8-mm diameter needle (15 gauge) was centered on the anterior commissure, and 2 plugs of tissue were punched from the slice. Plugs from three rats confirmed to be from the nucleus accumbens were pooled for microarray analyses. Animals were handled in accordance with the Guide for the Care and Use of Laboratory Animals as adopted and promulgated by the National Institutes of Health.

DNA Microarray Analyses—Pooled nucleus accumbens punches were stored at −80 °C in RNAlater™, a RNA stabilization reagent, until their total RNA was isolated. Total RNA was extracted, qualified, and quantified. Pooled total RNA (~2.5 μg) for each array was used for the mRNA amplification/labeling process. mRNA was reverse-transcribed using an oligo(dT) primer encoding a T7 RNA polymerase promoter to make cDNA. cDNA was then purified and transcribed into biotin-labeled cRNA. After purifying and quantifying the cRNA, the unfragmented transcript sizes were determined using an Agilent Bioanalyzer 2100. cRNA was fragmented, and the hybridization mix was applied to Affymetrix GeneChip® rat genome 230 2.0 arrays and hybridized to the 25-mers on the array. The Affymetrix Fluidics Station 450 was used for the wash and stain process. The GeneChip was washed to remove nonspecific hybridization. The three-step staining process was conducted as follows: 1) application of a streptavidin-phycoerythrin conjugate; 2) addition of biotinylated anti-streptavidin; and 3) second application of the streptavidin-phycoerythrin conjugate. This staining process allowed for fluorescent visualization of the oligonucleotide-cRNA hybrids. The arrays were scanned (Affymetrix GeneChip Scanner 3000), and the resulting raw image was converted to informative numerical data. The fluorescent signal was quantified, and relative transcript abundance was calculated. Microarray Suite 5.0 (MAS 5) algorithms from the Affymetrix GeneChip® operating software 1.2 were used to convert raw images to single chip analysis files that consist of signal intensities and detection calls for each probe. To determine labeling and hybridization efficiency, quality metrics from each chip were analyzed by producing report files that display scaling factor, background values, and 3′:5′ ratios of housekeeping and spike-in poly(A) labeling controls.

A *t*-statistic program called Cyber-T was used to conduct an efficient and robust statistical analysis to determine which of the 31,043 transcripts represented on the Rat 230 2.0 array are differentially expressed. Cyber-T analysis is *not* based on fold changes, instead, it relies on statistical significance (*p* value), modeling the standard deviation as a function of signal intensity, and therefore minimizes the false discovery rate by reducing the significance of probe sets at low signal intensities, even when their observed fold changes are high. Cyber-T then conducts a regularized *t* test, which uses a Bayesian estimate of variance among individual gene signal intensities within an experiment (64). See also the Cyber-T website. The entire analysis was performed on log-transformed data, and a p value ≤ 0.01 was set as the cutoff.

Thrombospondin1 Protein Assays—Cells were treated with morphine (1 μM), buprenorphine (1 μM), and/or naloxone (1 μM) or U0126 (1 μM) as described in the figure legends. After treatment, media were collected, and cells were washed with cold phosphate-buffered saline and then lysed with buffer containing 50 mM Tris hydrochloride, 0.25% sodium deoxycholate, 150 mM sodium chloride, 1 mM EGTA, 1% Nonidet P-40, 1 mM phenylmethylsulfonyl fluoride, 1 mM sodium orthovanadate, 1 mM sodium fluoride, 10 μg/ml aprotinin, 10 μg/ml leupeptin. After 15 min, lysates were spun at 14,000 × *g* for 10 min at 4 °C, and protein concentration of the supernatants was determined. Collected media were concentrated through 30-kDa molecular mass cutoff centrifuge concentrator (Millipore, Bedford, MA) following the manufacturer's instructions, and then protein concentration was determined. Cell lysates (30 μg of protein/lane) and concentrated media (100 μg of protein/lane) were

separated by 7.5% SDS-PAGE. Proteins were blotted on Immobilon P polyvinylidene difluoride membranes (Millipore). Nonspecific sites were blocked with 5% milk in Tris-buffered saline + 0.2% Tween 20 (TBST). Blots were then washed three times with TBST and incubated with anti-TSP1 Ab diluted 1:200 in 5% milk/TBST for 2.5 h at room temperature. After three washes with TBST, blots were incubated with 1:2000 diluted goat anti-mouse-IgG for 1 h at room temperature. Bands were visualized using an ECL chemiluminescence detection system from GE Healthcare and exposure to Classic Blue sensitive x-ray film (Molecular Technologies, St. Louis). Band intensities were determined by densitometric analysis using a Kodak DC120 digital camera, Kodak ds 1D version 3.0.2 software (Kodak Scientific Imaging System, New Haven, CT) and Scion Image software (Scion Corp., Frederick, MD).

In Vivo Drug Treatment for qRT-PCR Analysis—In single injection experiments, P5 Wistar rats were administered vehicle or 5 mg/kg morphine s.c. In repeated injection experiments, P5 Wistar rats were administered vehicle or 5 mg/kg morphine s.c. every 12 h for 2.5 days or once daily for 8 days. Then 6 or 24 h after the last injection, rats were anesthetized with halothane until comatose and killed by cervical decapitation. Brains were transferred on a brain slicer (Neuroscience Inc., Osaka, Japan), and a 2-mm slice of brain was made through levels of about 11 to 9 mm from the interaural line. The cortical region and limbic regions were dissected from the slices. These experiments were performed in accordance with Institutional Guidelines for the Care and Use of Experimental Animals that are in compliance with the UK Animals (Scientific Procedures) Act of 1986. All efforts were made to minimize animal suffering and to reduce the number of animals used.

qRT-PCR Analysis of Brain Tissue—To determine TSP-1 mRNA levels, total RNA was isolated using a Qiagen RNeasy mini kit (Qiagen, Valencia, CA) and quantified using spectrophotometer ND-1000 (NanoDrop Technologies, Inc, Wilmington, DE). On-column digestion of DNA was performed during RNA purification using the RNase-free DNase set (Takara Bio Inc., Shiga, Japan). The PrimeScript® RT reagent kit (Takara Bio Inc.) with random hexamer primers was used to reverse-transcribe 500 ng of total RNA to cDNA. Primers for TSP-1 and GAPDH were supplied by Takara Bio Inc. Primers were mixed with SYBR® Premix Ex TaqII (Takara Bio Inc.), and 3 μl of cDNA was added to 22 μl of the mix for each reaction, for a total volume of 25 μl. Real time PCR was performed on a Thermal Cycler Dice® real time system (TP800, Takara Bio Inc.) as follows: 95 °C for 30 s, followed by 40 cycles of denaturing at 95 °C for 5 s, and annealing at 60 °C for 30 s. Reaction specificity was confirmed by gel electrophoresis of RT-PCR product to identify bands of expected amplicon size, 88 bp for rat-TSP-1 and 143 bp for rat-GAPDH. In addition, a melting point analysis was performed for each run to confirm a product-specific melting point temperature. Sequences used were as follows: TSP1 primer forward, ATTGGCGATGCCTGTGATGA, and reverse, ACTGGGCAGGGTTGTAATGGAA; GAPDH primer forward, GGCACAGTCAAGGCTGAGAATG, and reverse, ATGGTGGTGAAGACGCCAGTA. Primer efficiencies were calculated by obtaining the slope of the graph of *Ct* values *versus* the log of the serial dilution values for the cDNA standard solution (10^7, 10^6, 10^5, 10^4, and 10^3 copies) for each primer. Efficiencies were calculated according to the equation: $E = 10(-1/\text{slope})$. Relative quantification was performed to assess fold changes in gene expression as described previously (65).

qRT-PCR Analysis of Astrocytes—To determine TSP1 mRNA levels in immortalized rat astrocytes, total RNA was isolated using a Qiagen RNeasy mini kit (Qiagen, Valencia, CA) and quantified using the NanoDrop spectrophotometer. On-column digestion of DNA was performed during RNA purification using the RNase-free DNase set (Qiagen). The Transcriptor First Strand cDNA synthesis kit (Roche Applied Science) with random hexamer primers was used to reverse transcribe 1 μg of total RNA to cDNA. Primers for TSP1 and GAPDH were designed using the Primer Express program (Applied Biosystems, Foster City, CA) and were supplied by Integrated DNA Technologies (Coralville, IA). Primers were mixed with SYBR Green I master mix (Roche Applied Science), and 5 μl of cDNA was added to 20 μl of the mix for each reaction, for a total volume of 25 μl. Real time PCR was performed on an Applied Biosystem 7500 PCR system as follows: 50 °C for 2 min, 95 °C for 10 min, followed by 40 cycles of denaturing at 95 °C for 15 s and annealing at 56 °C for 1 min. Reaction specificity was confirmed by gel electrophoresis of the RT-PCR product to identify bands of expected amplicon size, 51 bp for both rat-TSP1 and rat-GAPDH. In addition, a melting point analysis was performed for each run to confirm a product-specific melting point temperature. Primers used were as follows: TSP1 in astrocytes forward, 5′-TGGCATCATTTGCGGAGAG-3′, and reverse, 5′-TTTTCATTAGGCCAGCCGTC-3′; GAPDH forward, 5′-GTCCCCATCCCAACTCAGC-3′, and reverse, 5′-TGGAATTGTGAGGGAGATGCT-3′. Primer efficiencies were calculated by obtaining the slope of the graph of *Ct* values *versus* the log of the serial dilution values for the cDNA (1.00, 0.50, 0.25, and 0.13) for each primer. Efficiencies were calculated according to the equation: $E = 10(-1/\text{slope})$. Efficiencies were 2.03 and 2.18 for TSP1 and GAPDH, respectively. Relative quantification was performed to assess fold changes in gene expression as described previously (65).

Measurement of ERK Activity—Upon treatment with opioids, ERK phosphorylation was measured by immunoblotting as described previously (58). Blots were incubated with a phospho-ERK Ab (1:2000) overnight at 4 °C, followed by incubation with HRP-conjugated IgG (1:2000, Sigma) for 1 h at room temperature. Blots were also reprobed with an ERK Ab (1:1000), and the density of the bands was used as loading controls. Band intensities were determined by densitometry with a Kodak DC120 digital camera (Scientific Imaging Systems) and NIH ImageJ software. ERK stimulation in opioid- and/or and growth factor-treated cells was expressed as fold change over basal levels of ERK in control cells.

Immunofluorescence Confocal Laser Microscopy of Neuronal Cultures—Coverslips with attached neurons were fixed with PA and permeabilized as described previously (66). The following primary Abs were used: rabbit anti-synaptotagmin and mouse anti-PSD-95, both at 1:500 dilution and chicken anti MAP2 at 1:10,000 dilution. After remaining overnight at 4 °C, cells were incubated with fluorophore-conjugated secondary Abs: goat anti-rabbit Alexa 594, goat anti-mouse Alexa 488, and

aminomethylcoumarin acetate-conjugated anti-chicken IgY for 1–2 h at room temperature to label synaptotagmin, PSD, and neurons, respectively. In some cases, DAPI (1:200) was added with the secondary Abs. Cells were examined for immunofluorescence using an Olympus FV-1000 MPE confocal microscope and a water immersion ×20 (NA = 0.95) planachromatic objective lens operated at an optical zoom of ×2.5, with a 10-μs dwell time and a resolution of 1024 × 1024. Post image acquisition processing was carried out with ImageJ (National Institutes of Health) software.

Synapse Formation Quantification—Co-localized puncta appeared yellow on a dual emitting fluorescence channel due to merging of green (synaptotagmin) and red (PSD-95 staining). Images were counted, and the total number of puncta/neuron was estimated using ImageJ. Statistical differences between control and morphine-treated cells were determined using Student's *t* test or a one-way analysis of variance followed by the Newman-Keuls post hoc multiple comparison test. Puncta in at least 10 fields of cells on each of three separate coverslips were counted per experimental condition.

Images were also analyzed to determine the number of synapses per fixed dendrite length. Puncta per micrometer of dendrite was estimated using ImageJ software and custom plug-ins as described previously (34). To remove low frequency background from each image, the rolling ball background subtraction was applied. A threshold value for each color channel (synaptotagmin and PSD-95) was determined for each set of images/experiment. These values were then inserted into the plug-in program, and synapse formation was identified after merging the color channels. The number of synapses per 100 μm of dendrite length was quantified for each determinant. Two independent counts, one blinded, were made. The means of synapses per 100 μm of dendrite length for control and morphine-treated cells were presented.

Neurite Outgrowth Quantification—To determine dendrite length, MAP-2-stained neurons were measured using ImageJ. The scale of the images was obtained with the software of the Olympus FV-1000 MPE. For each image, total dendrite length was divided by the number of neurons in the field (67). Only dendrites that were connected to a soma were counted. Two independent counts, one blinded, were made, and the numbers of neurons counted per determinant were 178, 181, and 116.

RESULTS

Opiate Regulation of TSP1 Gene Expression in Vivo—Buprenorphine, a drug approved for the treatment of opiate dependence, is an opiate alkaloid that acts as a partial μ agonist. In previous studies, we found that chronic buprenorphine treatment of neonatal and adult rats down-regulated MOR binding and DAMGO-stimulated G protein coupling in their limbic and cortical regions (68). These transient neuroadaptations are thought to be a part of the signaling sequellae that initiate chronic changes in gene expression that both chronic opiates and other psychostimulants induce in regions such as the nucleus accumbens. This region possesses ample amounts of MOR as shown by studies in which methadone and buprenorphine-treated adult and neonatal rats were analyzed by binding and G protein coupling experiments (68, 69). Therefore, we undertook high throughput Affymetrics GeneChip expression array analyses of accumbens after chronic buprenorphine exposure to adult rats followed by spontaneous withdrawal, a model for human drug addiction (20). A total of 302 buprenorphine-responsive genes from the complete rat genome array (>30,000 transcripts) were expressed using rigorous statistical analysis ($\alpha = 0.01$; $n = 3$). A heat map of the microarray analysis is provided as supplemental material. Functional characterization of the genes revealed that a large number of those associated with synaptic plasticity were buprenorphine-responsive. In some cases, qRT-PCR was then used for verification purposes.

Based on qRT-PCR values, the astrocyte gliotransmitter TSP1 was shown to be down-regulated 4-fold by buprenorphine in the accumbens, whereas Homer1, PSD-95, and synaptotagmin1 were up-regulated (Fig. 1*A*). Chronic morphine treatment of rats followed by spontaneous withdrawal, the same regimen used for buprenorphine, also altered the expression of the latter three genes in the accumbens (20).

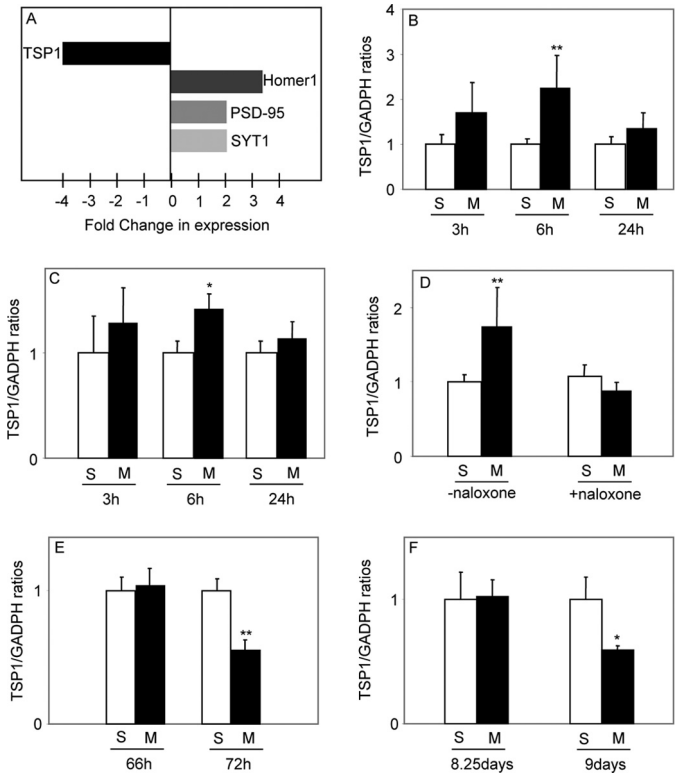

FIGURE 1. **Opiate regulation of TSP1 expression *in vivo*.** *A,* adult male rats were injected with buprenorphine (2.5 mg/kg/day, intraperitoneally) for 14 days and then allowed to undergo spontaneous withdrawal for 9 days. Nucleus accumbens were dissected from their brains, and its RNA was isolated and subjected to Affymetrix Chip analyses and qRT-PCR. Data on buprenorphine-induced down-regulation of TSP1 and up-regulation of Homer1, PSD-95, and synaptotagmin1 expression obtained by qRT-PCR are shown. *B,* P5 Wistar rat pups were injected s.c. with 5 mg/kg morphine for 3, 6, or 24 h, and cortical (*B*) and limbic (*C*) regions of their brains were dissected and their mRNA isolated. *, $p < 0.05$; **, $p < 0.01$, *versus* control; $n = 6–16$. *D,* P5 rats were also injected s.c. with 2 mg/kg naloxone for 10 min followed by 5 mg/kg morphine for 6 h, and cortical regions of their brains were dissected and their mRNA was isolated. **, $p < 0.01$, *versus* control; $n = 6–18$. *E,* P5 rats were injected twice daily with morphine (5 mg/kg s.c.) for 2 days and on the 3rd day were injected once, and 6 or 24 h later, cortical mRNA was isolated. $n = 5–6$. **, $p < 0.01$, *versus* control. *F,* P5 rats were injected daily with morphine (5 mg/kg s.c.) for 8 days, and 6 or 24 h later, cortical mRNA was isolated. $n = 5–10$. *, $p < 0.05$, *versus* control. *M,* morphine; *S,* saline.

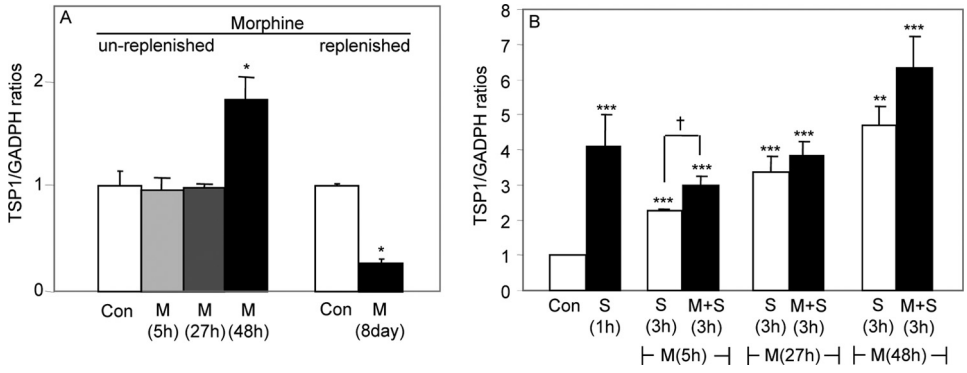

FIGURE 2. **Time course of morphine-induced changes in TSP1 gene expression in MOR1-transfected immortalized astrocytes.** *A,* cells were treated with either a single dose of morphine (1 μM) for 5, 27, and 48 h in the absence of serum or with morphine (1 μM) in media and serum daily for 8 days. Fresh media with serum but devoid of morphine were added for the last 24 h to the cells in the 8-day experiment. *, $p < 0.05$ *versus* control (*Con*), $n = 4$. *B,* cells were treated with a single dose of morphine (1 μM) for 5, 27, and 48 h and maintained in the presence of serum along with fresh morphine for the last 3 h. TSP1 gene expression was measured by qRT-PCR as described under "Experimental Procedures" normalizing with GAPDH for relative quantification. **, $p < 0.01$; ***, $p < 0.001$, *versus* control; †, $p < 0.05$ *versus* serum in the absence of morphine; $n = 4$–5. *M*, morphine; *S*, serum.

To determine whether morphine also modulated TSP1 expression *in vivo*, we conducted experiments in which P5 rat pups were injected with a single dose of morphine (5 mg/kg s.c.), and after 3, 6, and 24 h TSP1 mRNA levels were measured in cortical brain dissections (Fig. 1*B*). TSP1 levels are more readily detectable in neonatal rat brain than that of adults (10). TSP1 expression was increased 2-fold after 6 h of morphine administration but was not significantly different after 3 or 24 h. Similar morphine effects on TSP1 mRNA levels were found in limbic tissue (Fig. 1*C*). Preinjection with the antagonist naloxone reversed the stimulation by 6 h of morphine (Fig. 1*D*). These results suggest that morphine acts on MOR as its major target, but it may bind to KOR to a lesser extent as well (59). P5 rats were administered morphine every 12 h for 2.5 days and then sacrificed 6 or 24 h after a last injection. In rat pups sacrificed 24 h after the last injection (a total of 72 h), cortical TSP1 expression was down-regulated by 47% (Fig. 1*E*). In a longer chronic treatment regimen, P5 rats were injected with morphine daily for 8 days and then sacrificed 6 or 24 h later (Fig. 1*F*). A substantial inhibition (41%) was observed when expression was measured 24 h after the last injection.

Morphine Modulation of TSP1 Expression in Astrocytes—Given our *in vivo* results, we asked whether acute and chronic morphine treatment regimens of similar lengths could modulate TSP1 expression *in vitro*. Because TSPs are extracellular matrix proteins present on astrocytes that promote synapse formation (10), studies of these cells would facilitate delineation of the mechanism involved. To determine whether morphine treatment affects TSP1 gene expression, temporal features of morphine modulation of TSP1 mRNA levels in the absence or presence of serum were assayed by qRT-PCR. If MOR-transfected astrocytes were treated with a single dose of morphine for 5, 27, and 48 h in the absence of serum, TSP1 expression was essentially unchanged except for 48 h, wherein a slight increase was observed (Fig. 2*A*). However, if astrocytes were treated with morphine daily in serum-containing media for 8 days and then fresh media without morphine was maintained for 1 day, TSP1 expression was repressed by 81% (Fig. 2*A*). These results are consistent with *in vivo* findings (Fig. 1*F*). Serum alone stimulated TSP1 expression 2–4-fold in untransfected immortalized astrocytes at 1 and 3 h (Fig. 2*B*), a rapid induction also seen in other cells. However, after 6 and 24 h of serum treatment, changes in TSP1 mRNA were not observed (data not shown). If astrocytes were administered morphine for 5 h and serum for the last 3 h with fresh morphine, TSP1 mRNA levels were elevated by a modest 30% over serum-treated controls (Fig. 2*B*). This was consistent with the moderate increase in TSP1 expression *in vivo* (Fig. 1, *B* and *C*). In contrast, morphine treatment for 27 or 48 h with addition of serum for the last 3 h (along with fresh morphine) did not yield changes in TSP1 expression over serum alone again reminiscent of the animal studies (Fig. 1, *B* and *C*).

Opiates Down-regulate Astrocytic TSP1 Protein Levels via MOR and ERK in Astrocytes—Because acute morphine alone in the absence of serum did not influence TSP1 gene expression (Fig. 2*A*), we wished to determine how this opiate affected its protein levels. An immunoblot of TSP1 in control and morphine (5 min or 6 h)-treated astrocytes along with a human TSP1 standard show that the human protein migrates slightly faster than that of the rat (Fig. 3*A*) consistent with a previous report (70). Morphine (6 h) appeared to decrease TSP1 levels. Therefore, cellular and media TSP1 levels were measured after morphine exposure by immunoblotting under serum-deprived conditions in immortalized astrocytes. Time course studies revealed that 6 h after morphine addition, cellular levels of TSP1 were attenuated (Fig. 3*B*). By 24 h, cellular TSP1 protein had returned to levels that were slightly above control values, and TSP1 protein content in the media was reduced by almost 50%. By 48 h, cellular and media TSP1 protein had reverted back to control levels. It should be noted that neither morphine nor media was replenished in this experiment. These results suggested that acute morphine may be eliciting a TSP gene expression-independent inhibitory effect on TSP1 levels (Fig. 3*B*) that triggers a compensatory induction of TSP1 mRNA after 5–6 h of morphine exposure (Figs. 1, *B* and *C,* and 2*B*).

In immortalized astrocytes, co-transfected with both a MEK dominant negative mutant and MOR cDNA, morphine (6 h) failed to attenuate TSP1 protein levels, suggesting that acute actions of the opiate are ERK-mediated (Fig. 3*C*). Accordingly, MEK inhibitor U0126 blocked the down-regulation of cellular TSP1 levels by morphine (6 h) as well (Fig. 3*D*). Because U0126 was dissolved in DMSO, we ran control experiments with this solvent alone. Immortalized astrocytes were treated for 15 min or 6 or 25 h with the same volume of DMSO that was used in Fig. 3*D* ($n = 4$).

Immunoblot analysis showed that TSP1 levels in DMSO-treated lysates at all three time points did not differ from TSP1

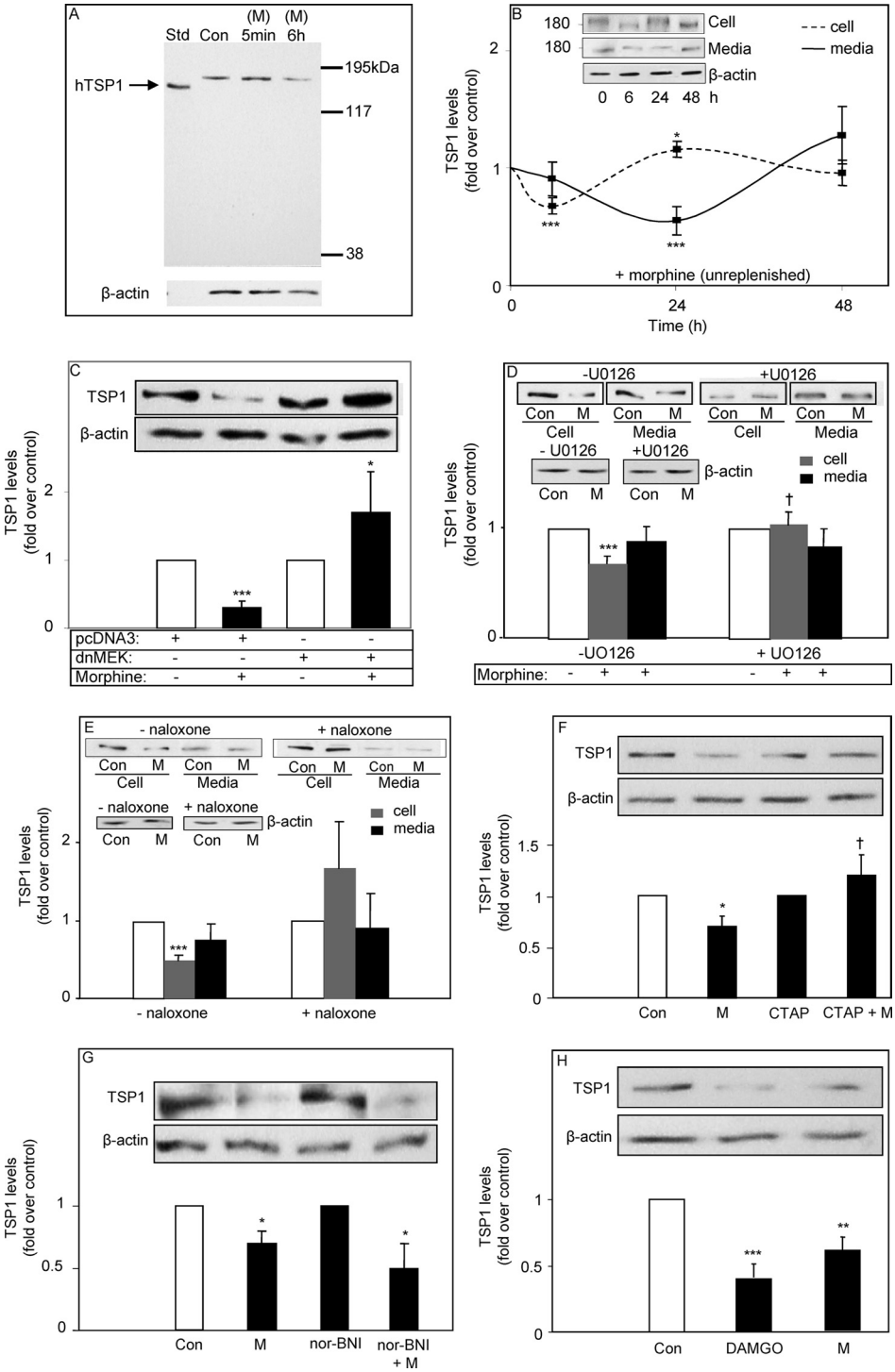

FIGURE 3. **Morphine-induced TSP1 protein down-regulation is attenuated by inhibition of ERK phosphorylation and MOR antagonism in MOR1-transfected immortalized astrocytes.** *A,* cells were maintained for 24 h in serum-free media and treated with morphine (1 μM) in media devoid of serum, and after 5 min or 6 h, their lysates were subjected to immunoblotting together with a human platelet-derived TSP1 standard. In these and the following TSP1 blots, gels are representative immunoblots showing TSP1 and β-actin. $n = 4–5$. *B,* cells were treated with morphine (1 μM) in media devoid of serum, and after 6, 24, or 48 h they were harvested. Cell lysates and media (passed through a filter with a 30-kDa cutoff) were subjected to immunoblotting on 7.5% SDS-polyacrylamide gels using a TSP1 monoclonal mouse Ab (1:200). The β-actin was run on cell blots only. Densitometry was performed on the band running at ~170 kDa consistent with the position of the human TSP1 standard. *, $p < 0.05$; ***, $p < 0.001$ *versus* control; $n = 5–20$. *C,* cells transiently co-transfected with MOR1 cDNA and either pcDNA3 vector or a dominant negative MEK pcDNA3 were treated with morphine (1 μM) for 6 h in media devoid of serum. *, $p < 0.05$; ***, $p < 0.001$ *versus* empty vector controls. $n = 4$. *D,* cells were treated with morphine (*M*) (1 μM) ± U0126 (1 μM) for 6 h in media devoid of serum. ***, $p < 0.001$ *versus* control (*Con*); †, $p < 0.05$ *versus* morphine in the absence of U0126; $n = 7–20$. *E,* cells were treated with morphine (1 μM) ± naloxone (1 μM) for 48 h in media devoid of serum but replenishing media with opiates every 24 h. Cells were then collected 24 h later. ***, $p < 0.001$ *versus* control; $n = 6–8$. *F,* cells were preincubated with CTAP (1 μM) for 1 h, followed by treatment with morphine (1 μM) for 6 h in media devoid of serum, and TSP1 levels were monitored. CTAP was replenished every 2 h during the morphine treatment. *, $p < 0.05$ *versus* control; †, $p < 0.05$ *versus* morphine; $n = 8$. *G,* cells were preincubated with nor-BNI (1 μM) for 1 h and treated with morphine (1 μM) for 6 h in media devoid of serum, and TSP1 levels were monitored. *, $p < 0.05$ *versus* corresponding control; $n = 10$. *H,* cells were treated daily with DAMGO (1 μM) or morphine (1 μM) for 8 days in media devoid of serum, and TSP1 levels were monitored. **, $p < 0.01$; ***, $p < 0.001$ *versus* control; $n = 12$.

protein in untreated lysates (data not shown). As seen in Fig. 3*E*, morphine down-regulated TSP1 levels by 50% after 48 h when it was replenished daily. Similarly, chronic buprenorphine (1 μM) depleted cellular TSP1 content by 50% after 48 h with daily replenishment ($p < 0.05$ *versus* control, $n = 6-8$). These data suggest that chronic (days) effects of morphine inhibit both TSP1 mRNA (Figs. 1, *E* and *F*, and 2*A*) and protein. The antagonist naloxone reversed the down-regulation of TSP1 levels by morphine in cells suggesting the involvement of MOR (Fig. 3*E*). Because naloxone is a general opioid receptor antagonist, we also tested the more selective and potent μ antagonist CTAP, which proved to reverse the action of morphine (Fig. 3*F*). CTAP was replenished every 2 h in these experiments as it is a small peptide that is susceptible to proteolysis by proteases secreted into media by astrocytes. Although morphine binds to KOR as well as MOR, the selective κ opioid antagonist, nor-BNI, did not block morphine attenuation of TSP1 levels (Fig. 3*G*). In addition, the prototypic μ agonist DAMGO significantly reduced TSP1 levels in MOR1-transfected immortalized astrocytes ($p < 0.01$, $n = 8$), and CTAP completely reversed the inhibitory actions of DAMGO (data not shown). Because the late passage immortalized astrocytes used were devoid of detectable endogenous MOR and KOR (61), transfected MOR1 is clearly the target of morphine, DAMGO, CTAP, and naloxone.

As seen in Fig. 2*A*, chronic morphine treatment for 8 days down-regulated TSP1 mRNA. Accordingly, we found significant decreases of 56 and 37% in TSP1 protein levels after 8 days of treatment of DAMGO and morphine, respectively (Fig. 3*H*).

Morphine Inhibits TGFβ1 Stimulation of ERK Phosphorylation in Astrocytes by Reducing TSP1 Levels—Similar to qRT-PCR findings with serum (Fig. 2*B*), a modest but significant ($p < 0.05$, $n = 5$) 2-fold induction of TSP1 mRNA was seen after 3 h of treatment with TGFβ1 in untransfected astrocytes but not after 1, 6, and 24 h of exposure (data not shown). When both immortalized and primary astrocytes were treated with TGFβ1 for 24 h, cellular TSP1 protein content was up-regulated 5- and 2-fold, respectively (Fig. 4, *A* and *B*). Morphine treatment (25 h) of immortalized astrocytes attenuated the up-regulation by serum 75% and by TGFβ1 63%. In primary astrocytes, morphine almost abolished TGFβ1-induced TSP1 level up-regulation under these conditions. Morphine alone had no effect after 25 h in serum-free media, similar to the findings for cellular TSP1 in Fig. 3*B*. MEK inhibitor U0126 reverted TGFβ1-induced TSP1 protein back to control levels implicating ERK in the growth factor mechanism (Fig. 4*C*).

Because TGFβ1 induced greater levels of TSP1 than controls, the inhibitory effects of morphine on TSP1 protein were more readily detectable. Therefore, we undertook additional studies on the actions of morphine on TGFβ1-induced TSP1 levels to amplify the changes that this opiate elicits in short periods. This would support our working hypothesis that TGFβ1 induced ERK activation by a mechanism involving EGFR transactivation, and morphine is capable of inhibiting this signaling. Therefore, we conducted ERK assays on astrocytes treated with TGFβ1 in the presence of the specific EGFR Tyr phosphorylation inhibitor AG1478 or acute morphine. As seen in Fig. 5, *A* and *B*, both AG1478 and morphine (2 h) greatly diminished TGFβ1-stimulated ERK phosphorylation in astrocytes. A question arose that an acute mechanism of opiate action may exist that is independent of TSP1 gene expression. One possibility would involve degradation of TSP1 by serving as a source of EGF-like ligands to transactivate EGFR. This mechanism was reported to occur either directly (71) or indirectly (72) depending on the cell type. Structure activity studies after site-specific mutagenesis established that TSP1 releases EGF-like repeats by an MMP-dependent mechanism, thereby reducing its levels. Function-blocking TSP1 Ab (C6.7) was shown to diminish TSP1-induced phosphorylation of EGFR. In previous EGFR transactivation studies on MOR signaling, we implicated MMP-mediated release of an extracellular source of EGF-like

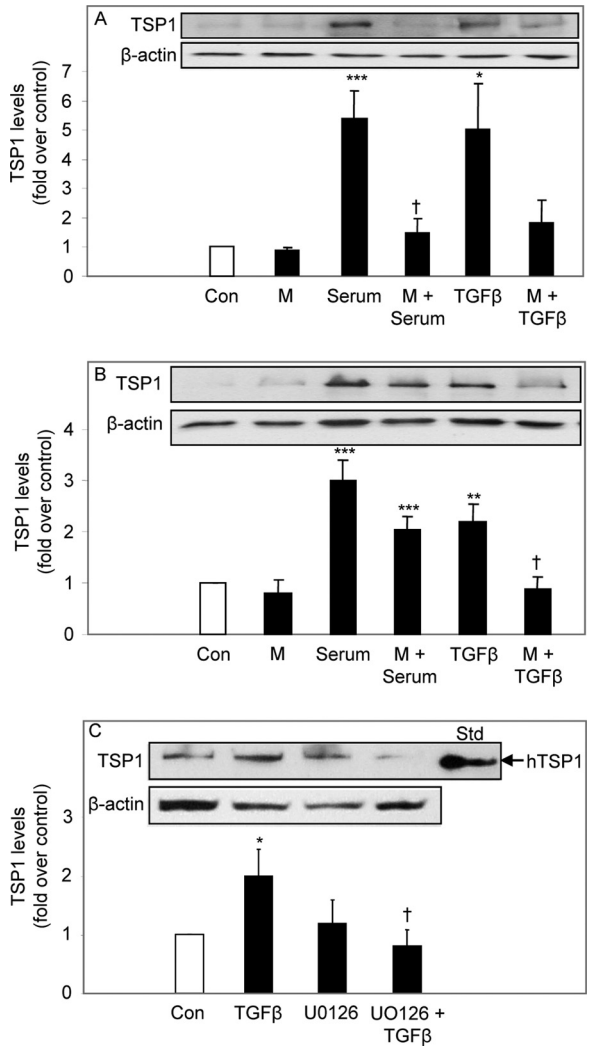

FIGURE 4. **Long term morphine attenuates TGFβ1- and serum-induced TSP1 protein up-regulation in astrocytes.** *A,* MOR1-transfected immortalized astrocytes were treated with 1 μM morphine (*M*) for 25 h. Alternatively, cells were pretreated with 1 μM morphine for 1 h, followed by addition of either serum (cell growth media) or TGFβ1 (1 ng/ml) for 24 h, and TSP1 levels were monitored. *Con*, control. *, $p < 0.05$; ***, $p < 0.001$ *versus* control. †, $p < 0.05$ *versus* their respective treatment in the absence of morphine; $n = 4-8$. *B,* primary astrocytes were treated with 1 μM morphine in the same manner as in Fig. 5*A* followed by serum or TGFβ1 (1 ng/ml) for 24 h, and TSP1 levels were assayed. **, $p < 0.01$; ***, $p < 0.001$ *versus* control. †, $p < 0.05$ *versus* their respective treatment in the absence of morphine; $n = 4-7$. *C,* MOR1 transfected cells were treated with TGFβ1 (1 ng/ml) ± U0126 (1 μM) for 24 h in media devoid of serum, and TSP1 levels were monitored. *, $p < 0.05$ *versus* control; †, $p < 0.05$ *versus* TGFβ1 alone $n = 8$.

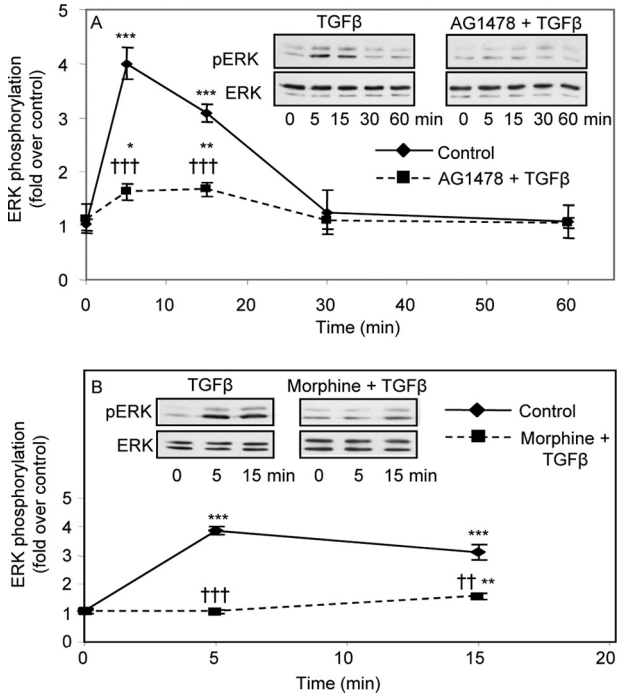

FIGURE 5. **Acute morphine and AG1478 attenuate TGFβ1-stimulated ERK phosphorylation in MOR1-transfected immortalized astrocytes.** *A,* cells were pretreated with 0.1 μM AG1478 for 20 min and treated with TGFβ1 (1 ng/ml) for 5, 15, 30, and 60 min in media devoid of serum, and ERK phosphorylation was assayed. Gels are representative immunoblots showing phosphorylated and total ERK1/2. *, $p < 0.05$; **, $p < 0.01$; ***, $p < 0.001$ *versus* control; †††, $p < 0.001$ *versus* TGFβ1 alone at the same time point; $n = 4$. *B,* cells were pretreated with 1 μM morphine for 2 h and treated with TGFβ1 (1 ng/ml) for 5 and 15 min, and ERK phosphorylation was assayed. Gels show phosphorylated and total ERK1/2. **, $p < 0.01$; ***, $p < 0.001$ *versus* control; ††, $p < 0.01$; †††, $p < 0.001$ *versus* their respective treatment in the absence of morphine; $n = 4$–5.

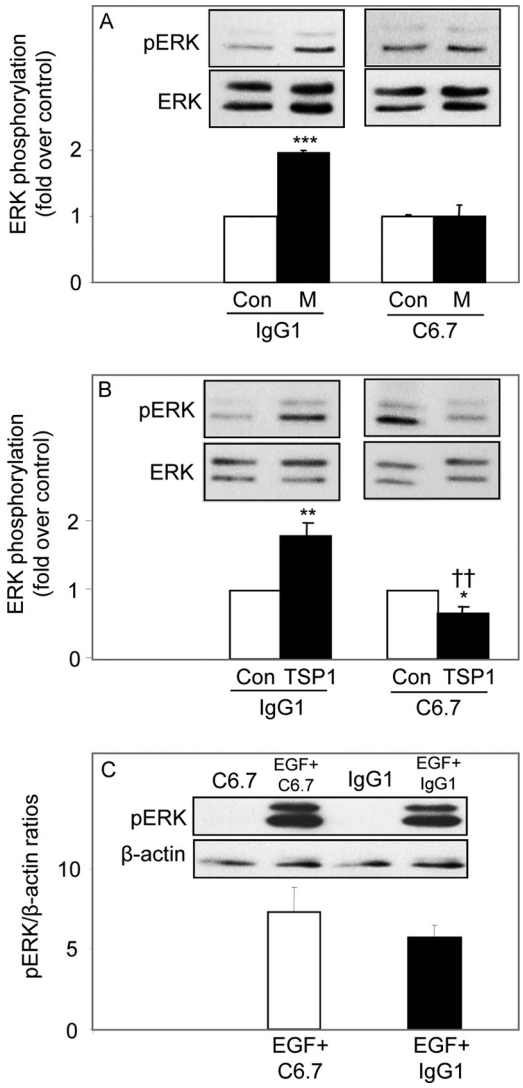

FIGURE 6. **TSP1-blocking Ab attenuates acute morphine, TSP1, but not EGF stimulation of ERK phosphorylation in immortalized astrocytes.** *A,* MOR-transfected cells were pretreated with 5 ng/ml of either a nonspecific IgG or TSP1 function-blocking antibody C6.7 for 1 h, treated without morphine (*Con*) or with 1 μM morphine (*M*), and ERK phosphorylation was assayed. ***, $p < 0.001$ *versus* control; $n = 4$. In these and the following blots of this figure, gels are representative immunoblots showing phosphorylated and total ERK1/2 or β-actin. *B,* cells were pretreated with 5 ng/ml of either a nonspecific IgG or C6.7 for 1 h and then treated with 5 μg/ml of human TSP1 for 5 min. *, $p < 0.05$; **, $p < 0.01$ *versus* control; ††, $p < 0.01$ *versus* treatment with TSP1 in the presence of IgG; $n = 6$. *C,* cells were pretreated with 5 ng/ml of either a nonspecific IgG or C6.7 for 1 h and then treated with 2.5 ng/ml EGF for 5 min; $n = 4$.

ligands in μ opioid-stimulated EGFR and ERK phosphorylation, but we did not identify the source of EGF-like ligands among the myriad of possibilities (56). To this end, we measured acute morphine-induced ERK phosphorylation in the presence of the function-blocking TSP1 Ab C6.7 (72). As seen in Fig. 6*A*, anti-TSP1 Ab C6.7 abolished morphine stimulation of ERK phosphorylation. A control IgG1 isotype-matched Ab did not affect morphine activation of ERK. Accordingly, TSP1 stimulated ERK phosphorylation, and this activation was abolished by C6.7 Ab (Fig. 6*B*). As a negative control, we showed that C6.7 Ab did not affect EGF-stimulated ERK activation (Fig. 6*C*).

Chronic Morphine Inhibits Neurite Outgrowth and Synaptic Puncta Formation in Astrocyte-Neuron Co-cultures—To determine cellular responses to chronic morphine, we prepared co-cultures of primary rat cortical astrocytes and rat hippocampal neurons, and the neurons were subjected to immunofluorescence confocal microscopy after 8–9 days of treatment. As shown in Fig. 7*A*, neurons were stained with presynaptic synaptotagmin (*green*), postsynaptic PSD-95 (*red*), and neuronal MAP2 (*blue*) markers. Synapses were identified by co-localization of the markers (merge). Neuron-astrocyte co-cultures were grown for 8–9 days; neurons were stained, and the number of puncta/neuron was counted. Control levels were about 8 puncta/neuron (Fig. 7*B*), which are comparable with values previously reported for retinal ganglion neurons that were also relatively immature and grown in heterochronic co-cultures with astrocytes (10, 34). These density values also reflect the fact that counts of puncta are taken in a relatively thin plane at the center of the neuron, and *z* stacking of images would yield higher values. Our counting data indicated that chronic morphine treatment of the co-cultures reduced synaptic puncta/neuron by 54% (Fig. 7*B*).

We also observed that the morphine-treated neurons displayed a reduction in the elongation of dendrites compared with controls in the co-cultures (Fig. 7*C*), consistent with previous reports that morphine suppresses neurite outgrowth in primary neuron cultures. The effect of morphine on neurite outgrowth was quantified by measuring total dendrite length/

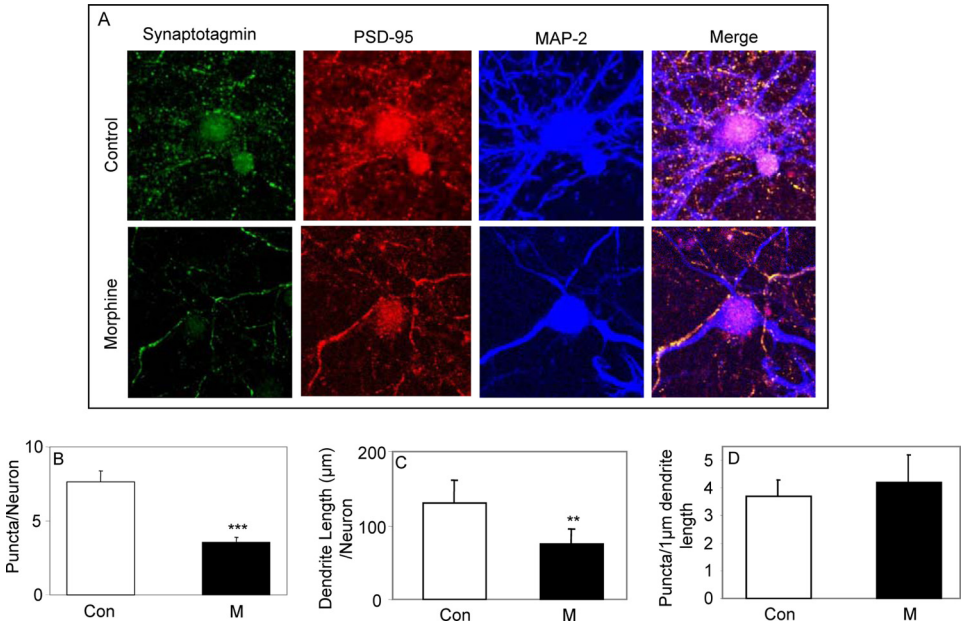

FIGURE 7. **Chronic morphine inhibits neurite outgrowth and synaptic puncta densities in astrocyte neuron co-cultures.** E18 rat hippocampal neurons were cultured on coverslips in companion 24-well plates with inserts containing P1 rat primary cortical astrocytes (see "Experimental Procedures"). Co-cultures were grown in neuronal maintenance media for 8–9 days, and 1 μM morphine was supplied on a daily basis. *A,* neurons were stained with rabbit anti-synaptotagmin, mouse anti-PSD95, and chicken anti-MAP2 Abs, followed by incubation with goat anti-rabbit Alexa 488 Ab (Molecular Probes), goat anti-mouse Alexa 594, and aminomethylcoumarin acetate-conjugated anti-chicken IgY, respectively. Coverslips were treated with anti-fade reagent and examined for immunofluorescence with an OLYMPUS FV-1000 MPE confocal microscope. ImageJ software was used to merge *red* and *green* images to detect synaptic puncta (*yellow*). *B,* quantification of puncta/neuron. ***, $p < 0.001$; $n = 4$. *C,* quantification of micrometers of dendrite/neuron. **, $p < 0.01$, $n = 3$. *D,* quantification of puncta per 100 μm of dendrite by custom plug-in software. $n = 3$. *Con*, control; *M*, morphine.

neuron. A 42% difference in dendrite elongation between controls and morphine-treated neurons was observed. The data suggest that neurite outgrowth could account for 71% of the total reduction of synapse formation in co-cultures with astrocytes. This observation raises the possibility that morphine diminished synapse formation primarily by attenuating neurite outgrowth. If this were the case, then the density of synaptic puncta per fixed length of dendrite in morphine-treated co-cultures should not differ from untreated cells. Measurements of this parameter revealed that puncta density did not vary (Fig. 7*D*). These findings clearly indicate that the reduction in neurite outgrowth diminishes synapse formation. Nevertheless, given the fact that TSP1 supports neurite outgrowth (35), our data do not rule out the possibility that morphine inhibition of TSP1 levels contributes directly to the reduction in both neurite outgrowth as well as in synapse formation.

DISCUSSION

Upon chronic treatment of adult rats with the opiate buprenorphine followed by spontaneous withdrawal, TSP1 expression in their nucleus accumbens was shown to be down-regulated 4-fold. To determine whether morphine also modulated TSP1 expression, we chose to use neonatal rats as their levels of TSP1/2 are much higher. Moreover, we wished to examine mechanistic aspects with primary rat astrocyte cultures and immortalized astrocytes that were derived from P1 pups. Therefore, the use of P5 pups would ensure better comparisons than adults between parallel *in vitro* and *in vivo* experiments. If P5 rat pups were treated with morphine for 6 h, a 2-fold increase in TSP1 gene expression was observed. However, if the pups were treated with morphine twice daily for 2.5 days or once daily for 8 days similar to the time course in the co-culture studies, TSP1 expression was diminished by 47 and 41%, respectively. Because TSP1 is synthesized primarily in astrocytes, we undertook experiments to further characterize the mechanism of modulation of TSP1 expression by opiates with these cells *in vitro*. The acute stimulatory action of morphine on TSP1 gene expression *in vivo* (Fig. 1, *B–D*) was also observed in astrocytes upon 5 h of exposure to morphine (Fig. 2*B*). Because acute (5 min) morphine induces ERK phosphorylation (57), it is possible that ERK mediates TSP1 mRNA up-regulation.

We then asked whether morphine was capable of stimulating TSP1 protein levels as measured by immunoblotting, but instead we discovered that cellular depletion of TSP1 occurred after short term (6 h) and chronic (2 and 8 days) treatment of astrocytes. This raised the possibility that the acute inhibitory action of morphine on TSP1 levels may include degradation of TSP1 by MMP/ADAM-induced limited proteolysis. Recently, it was shown that TSP1 can serve as a source of EGF-like ligands that may transactivate EGFR directly or indirectly by an MMP-dependent mechanism (71, 72). Accordingly, we found that a TSP1 function-blocking Ab inhibited acute (5 min) morphine or TSP1-stimulated ERK activation (Fig. 6). The depletion of TSP1 in this manner may turn on a compensatory stimulation of transcription of this extracellular matrix protein observed in the short term (5–6 h) treatment (Figs. 1, *B* and *C,* and 2*B*).

The mechanism of the inhibitory action of morphine on cellular TSP1 levels entailed mediation of MOR and ERK. The involvement of MOR was documented by the use of selective μ (CTAP) and κ (nor-BNI) opioid antagonists and the prototypic μ agonist DAMGO to mimic the actions of acute (6 h) and chronic (8 days) morphine. In previous studies of MOR signaling in astrocytes, we learned that ERK activation featured $G_{i/o}$ protein, CaM, and β-arrestin2-dependent pathways, all of which included EGFR transactivation (59). Although the G protein and β-arrestin2-dependent pathways were shown to be involved in astrocyte proliferation, CaM signaling was not, thereby making it a candidate for another cellular response and possibly TSP1 modulation.

There is evidence that TGFβ is capable of inducing TSP1 levels and/or expression in various cell lines, including astrocytes (36–40). In addition, TGFβ can modulate transcription of immediate early genes in a process mediated by EGFR trans-

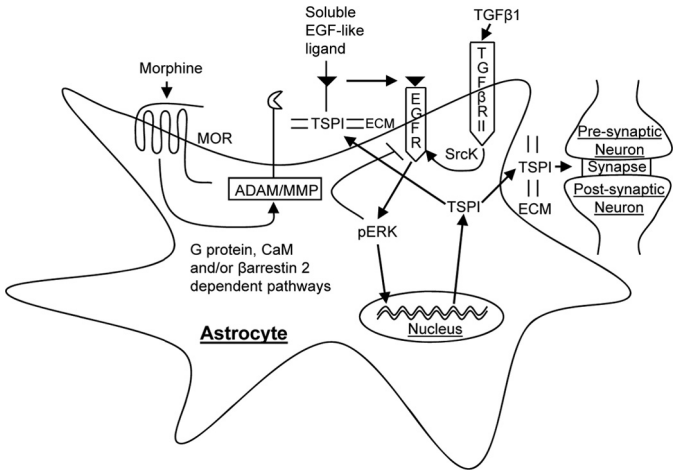

FIGURE 8. **Hypothetical model of morphine-induced reduction of TSP1 levels via TGFβ1 and its impact on synapse formation.** Acute morphine acts via MOR to activate EGFR in astrocytes. The transactivation of EGFR occurs upon MMP/ADAM-mediated release of EGF-like ligands from proteins either anchored to the plasma membrane or in the extracellular matrix (*ECM*). If TSP1, which contains EGF-like domains, is a substrate of the MMP/ADAM, it will be depleted. Upon chronic morphine treatment, phospho-ERK (*pERK*) formed by transactivation phosphorylates Ser residues of EGFR and that leads to its endocytosis that by $\geq$2 h is detectable. This down-regulation of EGFR diminishes TGFβ1-induced TSP1 *de novo* synthesis. The final outcome of the decreases in TSP1 by limited proteolysis and inhibition of TSP1 synthesis via a different phospho-ERK pathway is a reduction of neurite outgrowth and synapse formation elicited by this gliotransmitter.

activation and ERK phosphorylation (41, 73). Therefore, we addressed the question of whether morphine treatment attenuated TGFβ-induced TSP1 levels. As seen in Fig. 4, this proved to be the case in both immortalized and primary astrocytes. Evidence for ERK mediation of TGFβ induction of TSP1 levels was also obtained. In these experiments, TGFβ1 alone induced a 5-fold change in TSP1 levels after 24 h. This suggested that TGFβ1 induced TSP1 expression under conditions used with primary and immortalized cortical astrocytes, and this was verified by qRT-PCR experiments in which TGFβ induced a 2-fold increase in TSP1 expression after 3 h in immortalized astrocytes. We also discovered here that both acute (2 h) morphine and AG1478, a specific inhibitor of EGFR Tyr phosphorylation, strongly attenuated TGFβ activation of ERK (Fig. 5).

Because both TGFβ1 and morphine modulate TSP1 protein levels via EGFR and ERK activation, an attractive hypothesis is that EGFR is at the point of convergence of these two pathways and is the target of chronic morphine inhibitory action on TSP1 synthesis (Fig. 8). In earlier studies, we obtained evidence suggesting that μ opioid signaling can inhibit EGF stimulation of ERK and thereby astrocyte proliferation by a negative feedback loop mechanism, wherein EGFR is phosphorylated by ERK at Ser residues (56, 59). EGFR is known to be down-regulated via internalization and lysosomal degradation upon Ser phosphorylation. To detect this feedback inhibition, morphine exposure had to be maintained for over 1 h and it persisted for over 3 h, suggesting it could explain the acute (hour) inhibitory effect of this opiate on TSP1 protein levels. These results exemplify temporally distinct μ opioid modulation of ERK activation. However, the data do not rule out the possibility that morphine and TGFβ may activate populations of ERK that are known to occur in different compartments such as clathrin-coated pits or endosomes in astrocytes. There is ample precedence for such spatially discrete sites of ERK activation, as shown in many cell types by a number of research groups and in astrocytes by our group (58, 59 and references cited therein).

It is also possible that morphine can acutely deplete TSP1 as suggested in Fig. 6. Because μ and κ opioids also appear to transactivate EGFR by stimulating the release of EGF-like repeats by an MMP-dependent mechanism in astrocytes (56), this opiate may promote limited proteolysis of TSP1 to release its three EGF-like repeats as well (Fig. 8). Additional studies are underway to show that acute treatment with morphine can deplete TSP1 levels by this mechanism in astrocytes. In conclusion, evidence gained thus far is consistent with the notion that both acute and chronic morphine reduce TSP1 levels in astrocytes by mechanisms implicating transactivation of the important receptor, EGFR. However, in the experiment with mature rats that entail 14 days of chronic morphine followed by 9 days of withdrawal, results of the array analysis would only reflect the actions of the chronic morphine mechanism as influenced by withdrawal. After 9 days of abstinence, residual morphine would be depleted, thereby eliminating occurrence of acute actions.

Because chronic morphine and DAMGO reduced astrocyte media TSP1 levels by 37 and 56%, we sought to determine the impact of this inhibition on synapse formation and neurite outgrowth in astrocyte neuron co-cultures as both cellular responses are potentiated by TSP1 (10, 35). Upon growing co-cultures for 8–9 days in the presence of morphine (replenished daily), we determined by immunofluorescence confocal microscopy that synaptic puncta/neuron and dendrite length (micrometer) were reduced by 54 and 43%, respectively. To determine whether the reduction of dendrite elongation contributed to the loss of synaptic puncta, we also measured puncta density (puncta/1 μm dendrite length) and found no change between puncta densities in treated and control cells. The data suggest that 71% of the puncta loss was caused primarily by reduction in neurite outgrowth. It is possible then that 29% of the puncta loss may be due to a direct action of morphine on astrocyte-driven synapse formation. TSP1 also stimulates neurite formation *in vivo* and *in vitro*. In addition, function-blocking TSP1 Abs diminish neurite outgrowth (32). Finally, it is known that addition of astrocytes to primary neurons enhances neurite outgrowth (74). Therefore, morphine may decrease neurite formation by depleting TSP1 secreted by astrocytes in primary neuron cultures. It has been known for some time that opioids modulate neurites and dendritic spines of neurons (75–82). The data indicate that opioids can influence neurite outgrowth positively and negatively depending upon dosage and other factors, but the mechanism of action has not been examined. Studies on neurite outgrowth and other changes in neuronal morphology have provided indirect evidence for an interrelationship between opioids and synaptogenesis. However, primary neurons are not generally known to express TSP1 with a few exceptions (83, 84). This gliotransmitter may originate from residual astrocytes in primary neuronal cultures. This may be possible as recently homogeneous neuronal populations were shown to be difficult to prepare unless immunopanning is used in their purification (42). Morphine treatment of Neuro2A

cells also modulates neurite outgrowth (79). However, these neuroblastoma cells may express TSP1, as transformed cells express many genes not found in their wild type counterparts. Neurons derived from embryonic carcinoma cells express TSP1 (83). Experiments are underway to determine whether TSP1 is directly involved in the mechanism of inhibition of both neurite outgrowth and synapse formation by morphine *in vitro* and *in vivo*. In these studies, adult rats will also be treated with chronic opiates followed by spontaneous withdrawal, the regimen used in the buprenorphine gene profiling experiments (Fig. 1*A*). It is generally agreed that neural adaptations implicated in addiction by many drugs, including opiates, are brought about by modification of synaptic plasticity mechanisms that can feature neuronal glia interactions (85–87). Therefore, the TSP1-dependent mechanism suggested here (Fig. 8) may prove to be a novel example of disruption of synaptic plasticity in opiate addiction.

Acknowledgments—We are indebted to Dr. E. Krebs for the MEK1a K97A/pCDNA3 and control vector containing plasmids and Dr. Fernanda Laezza (Department of Pharmacology and Toxicology, University of Texas Medical Branch, Galveston) for many helpful discussions and expert assistance in growing astrocyte neuron co-cultures.

REFERENCES

1. Blondel, O., Collin, C., McCarran, W. J., Zhu, S., Zamostiano, R., Gozes, I., Brenneman, D. E., and McKay, R. D. (2000) *J. Neurosci.* **20,** 8012–8020
2. Parpura, V., and Haydon, P. G. (2000) *Proc. Natl. Acad. Sci. U.S.A.* **97,** 8629–8634
3. Haydon, P. G. (2001) *Nat. Rev. Neurosci.* **2,** 185–193
4. Parpura, V., Basarsky, T. A., Liu, F., Jeftinija, K., Jeftinija, S., and Haydon, P. G. (1994) *Nature* **369,** 744–747
5. Ullian, E. M., Sapperstein, S. K., Christopherson, K. S., and Barres, B. A. (2001) *Science* **291,** 657–661
6. Hansson, E., and Rönnbäck, L. (2003) *FASEB J.* **17,** 341–348
7. Fields, R. D., and Stevens, B. (2000) *Trends Neurosci.* **23,** 625–633
8. Panatier, A., Theodosis, D. T., Mothet, J. P., Touquet, B., Pollegioni, L., Poulain, D. A., and Oliet, S. H. (2006) *Cell* **125,** 775–784
9. Yang, Y., Ge, W., Chen, Y., Zhang, Z., Shen, W., Wu, C., Poo, M., and Duan, S. (2003) *Proc. Natl. Acad. Sci. U.S.A.* **100,** 15194–15199
10. Christopherson, K. S., Ullian, E. M., Stokes, C. C., Mullowney, C. E., Hell, J. W., Agah, A., Lawler, J., Mosher, D. F., Bornstein, P., and Barres, B. A. (2005) *Cell* **120,** 421–433
11. Stevens, B., Allen, N. J., Vazquez, L. E., Howell, G. R., Christopherson, K. S., Nouri, N., Micheva, K. D., Mehalow, A. K., Huberman, A. D., Stafford, B., Sher, A., Litke, A. M., Lambris, J. D., Smith, S. J., John, S. W., and Barres, B. A. (2007) *Cell* **131,** 1164–1178
12. Ishibashi, T., Dakin, K. A., Stevens, B., Lee, P. R., Kozlov, S. V., Stewart, C. L., and Fields, R. D. (2006) *Neuron* **49,** 823–832
13. Beattie, E. C., Stellwagen, D., Morishita, W., Bresnahan, J. C., Ha, B. K., Von Zastrow, M., Beattie, M. S., and Malenka, R. C. (2002) *Science* **295,** 2282–2285
14. Murai, K. K., Nguyen, L. N., Irie, F., Yamaguchi, Y., and Pasquale, E. B. (2003) *Nat. Neurosci.* **6,** 153–160
15. Jiao, J. W., Feldheim, D. A., and Chen, D. F. (2008) *Proc. Natl. Acad. Sci. U.S.A.* **105,** 8778–8783
16. Nishida, H., and Okabe, S. (2007) *J. Neurosci.* **27,** 331–340
17. Xu, J., Xiao, N., and Xia, J. (2010) *Nat. Neurosci.* **13,** 22–24
18. Jones, S., and Bonci, A. (2005) *Curr. Opin. Pharmacol.* **5,** 20–25
19. Jacobs, E. H., Spijker, S., Verhoog, C. W., Kamprath, K., de Vries, T. J., Smit, A. B., and Schoffelmeer, A. N. (2002) *FASEB J.* **16,** 1961–1963
20. Spijker, S., Houtzager, S. W., de Gunst, M. C., de Boer, W. P., Schoffelmeer, A. N., and Smit, A. B. (2004) *FASEB J.* **18,** 181–208
21. Van den Oever, M. C., Goriounova, N. A., Li, K. W., Van der Schors, R. C., Binnekade, R., Schoffelmeer, A. N., Mansvelder, H. D., Smit, A. B., Spijker, S., and De Vries, T. J. (2008) *Nat. Neurosci.* **11,** 1053–1058
22. Ammon-Treiber, S., and Höllt, V. (2005) *Addict. Biol.* **10,** 81–89
23. Ziolkowska, B., Gieryk, A., Bilecki, W., Wawrzczak-Bargiela, A., Wedzony, K., Chocyk, A., Danielson, P. E., Thomas, E. A., Hilbush, B. S., Sutcliffe, J. G., and Przewlocki, R. (2005) *J. Neurosci.* **25,** 4996–5003
24. Suzuki, M., Narita, M., Narita, M., and Suzuki, T. (2006) *Eur. J. Pharmacol.* **535,** 166–168
25. Morón, J. A., Abul-Husn, N. S., Rozenfeld, R., Dolios, G., Wang, R., and Devi, L. A. (2007) *Mol. Cell. Proteomics* **6,** 29–42
26. Hemby, S. E. (2004) *Neuroscience* **126,** 689–703
27. Adams, J. C. (2001) *Annu. Rev. Cell Dev. Biol.* **17,** 25–51
28. Adams, J. C., and Lawler, J. (2004) *Int. J. Biochem. Cell Biol.* **36,** 961–968
29. O'Shea, K. S., Rheinheimer, J. S., and Dixit, V. M. (1990) *J. Cell Biol.* **110,** 1275–1283
30. O'Shea, K. S., Liu, L. H., and Dixit, V. M. (1991) *Neuron* **7,** 231–237
31. Neugebauer, K. M., Emmett, C. J., Venstrom, K. A., and Reichardt, L. F. (1991) *Neuron* **6,** 345–358
32. Osterhout, D. J., Frazier, W. A., and Higgins, D. (1992) *Dev. Biol.* **150,** 256–265
33. Ullian, E. M., Christopherson, K. S., and Barres, B. A. (2004) *Glia* **47,** 209–216
34. Barker, A. J., Koch, S. M., Reed, J., Barres, B. A., and Ullian, E. M. (2008) *J. Neurosci.* **28,** 8150–8160
35. Yu, K., Ge, J., Summers, J. B., Li, F., Liu, X., Ma, P., Kaminski, J., and Zhuang, J. (2008) *PLoS ONE* **3,** e2470
36. Scott-Drew, S., and ffrench-Constant, C. (1997) *J. Neurosci. Res.* **50,** 202–214
37. Cambier, S., Gline, S., Mu, D., Collins, R., Araya, J., Dolganov, G., Einheber, S., Boudreau, N., and Nishimura, S. L. (2005) *Am. J. Pathol.* **166,** 1883–1894
38. Fuchshofer, R., Birke, M., Welge-Lussen, U., Kook, D., and Lütjen-Drecoll, E. (2005) *Invest. Ophthalmol. Vis. Sci.* **46,** 568–578
39. Nakagawa, T., Lan, H. Y., Glushakova, O., Zhu, H. J., Kang, D. H., Schreiner, G. F., Böttinger, E. P., Johnson, R. J., and Sautin, Y. Y. (2005) *J. Am. Soc. Nephrol.* **16,** 899–904
40. Dibrov, A., Kashour, T., and Amara, F. M. (2006) *Growth Factors* **24,** 1–11
41. Joo, C. K., Kim, H. S., Park, J. Y., Seomun, Y., Son, M. J., and Kim, J. T. (2008) *Oncogene* **27,** 614–628
42. Cahoy, J. D., Emery, B., Kaushal, A., Foo, L. C., Zamanian, J. L., Christopherson, K. S., Xing, Y., Lubischer, J. L., Krieg, P. A., Krupenko, S. A., Thompson, W. J., and Barres, B. A. (2008) *J. Neurosci.* **28,** 264–278
43. Barg, J., Belcheva, M. M., Bem, W. T., Lambourne, B., McLachlan, J. A., Tolman, K. C., Johnson, F. E., and Coscia, C. J. (1991) *Peptides* **12,** 845–849
44. Stiene-Martin, A., Gurwell, J. A., and Hauser, K. F. (1991) *Brain Res. Dev. Brain Res.* **60,** 1–7
45. Ruzicka, B. B., Fox, C. A., Thompson, R. C., Meng, F., Watson, S. J., and Akil, H. (1995) *Brain Res. Mol. Brain Res.* **34,** 209–220
46. Gurwell, J. A., Duncan, M. J., Maderspach, K., Stiene-Martin, A., Elde, R. P., and Hauser, K. F. (1996) *Brain Res.* **737,** 175–187
47. Stiene-Martin, A., Knapp, P. E., Martin, K., Gurwell, J. A., Ryan, S., Thornton, S. R., Smith, F. L., and Hauser, K. F. (2001) *GLIA* **36,** 78–88
48. Hauser, K. F., and Mangoura, D. (1998) *Perspect. Dev. Neurobiol.* **5,** 437–449
49. Xu, M., Bruchas, M. R., Ippolito, D. L., Gendron, L., and Chavkin, C. (2007) *J. Neurosci.* **27,** 2570–2581
50. Bruchas, M. R., Macey, T. A., Lowe, J. D., and Chavkin, C. (2006) *J. Biol. Chem.* **281,** 18081–18089
51. Eriksson, P. S., Hansson, E., and Rönnbäck, L. (1990) *Neurochem. Res.* **15,** 1123–1126
52. Eriksson, P. S., Hansson, E., and Rönnbäck, L. (1991) *Neuropharmacology* **30,** 1233–1239
53. Barg, J., Belcheva, M. M., Zimlichman, R., Levy, R., Saya, D., McHale, R. J., Johnson, F. E., Coscia, C. J., and Vogel, Z. (1994) *J. Neurosci.* **14,** 5858–5864
54. Bohn, L. M., Belcheva, M. M., and Coscia, C. J. (2000) *J. Neurochem.* **74,**

564–573
55. Belcheva, M. M., Haas, P. D., Tan, Y., Heaton, V. M., and Coscia, C. J. (2002) *J. Pharmacol. Exp. Ther.* **303,** 909–918
56. Belcheva, M. M., Tan, Y., Heaton, V. M., Clark, A. L., and Coscia, C. J. (2003) *Mol. Pharmacol.* **64,** 1391–1401
57. Belcheva, M. M., Clark, A. L., Haas, P. D., Serna, J. S., Hahn, J. W., Kiss, A., and Coscia, C. J. (2005) *J. Biol. Chem.* **280,** 27662–27669
58. McLennan, G. P., Kiss, A., Miyatake, M., Belcheva, M. M., Chambers, K. T., Pozek, J. J., Mohabbat, Y., Moyer, R. A., Bohn, L. M., and Coscia, C. J. (2008) *J. Neurochem.* **107,** 1753–1765
59. Miyatake, M., Rubinstein, T. J., McLennan, G. P., Belcheva, M. M., and Coscia, C. J. (2009) *J. Neurochem.* **110,** 662–674
60. Radany, E. H., Brenner, M., Besnard, F., Bigornia, V., Bishop, J. M., and Deschepper, C. F. (1992) *Proc. Natl. Acad. Sci. U.S.A.* **89,** 6467–6471
61. Kim, E., Clark, A. L., Kiss, A., Hahn, J. W., Wesselschmidt, R., Coscia, C. J., and Belcheva, M. M. (2006) *J. Biol. Chem.* **281,** 33749–33760
62. McCarthy, K. D., and de Vellis, J. (1980) *J. Cell Biol.* **85,** 890–902
63. Laezza, F., Gerber, B. R., Lou, J. Y., Kozel, M. A., Hartman, H., Craig, A. M., Ornitz, D. M., and Nerbonne, J. M. (2007) *J. Neurosci.* **27,** 12033–12044
64. Long, A. D., Mangalam, H. J., Chan, B. Y., Tolleri, L., Hatfield, G. W., and Baldi, P. (2001) *J. Biol. Chem.* **276,** 19937–19944
65. Pfaffl, M. W. (2001) *Nucleic Acids Res.* **29,** 2002–2007
66. Ullian, E. M., Harris, B. T., Wu, A., Chan, J. R., and Barres, B. A. (2004) *Mol. Cell. Neurosci.* **25,** 241–251
67. Harper, J. M., Krishnan, C., Darman, J. S., Deshpande, D. M., Peck, S., Shats, I., Backovic, S., Rothstein, J. D., and Kerr, D. A. (2004) *Proc. Natl. Acad. Sci. U.S.A.* **101,** 7123–7128
68. Hou, Y., Tan, Y., Belcheva, M. M., Clark, A. L., Zahm, D. S., and Coscia, C. J. (2004) *Brain Res. Dev. Brain Res.* **151,** 149–157
69. Hou, Y., Belcheva, M. M., Clark, A. L., Zahm, D. S., and Coscia, C. J. (2006) *Neurosci. Lett.* **395,** 244–248
70. Tikhonenko, A. T., Black, D. J., and Linial, M. L. (1996) *J. Biol. Chem.* **271,** 30741–30747
71. Liu, A., Mosher, D. F., Murphy-Ullrich, J. E., and Goldblum, S. E. (2009) *Microvasc. Res.* **77,** 13–20
72. Liu, A., Garg, P., Yang, S., Gong, P., Pallero, M. A., Annis, D. S., Liu, Y., Passaniti, A., Mann, D., Mosher, D. F., Murphy-Ullrich, J. E., and Goldblum, S. E. (2009) *J. Biol. Chem.* **284,** 6389–6402
73. Semlali, A., Jacques, E., Plante, S., Biardel, S., Milot, J., Laviolette, M., Boulet, L. P., and Chakir, J. (2008) *Am. J. Respir. Cell Mol. Biol.* **38,** 202–208
74. van den Pol, A. N., and Spencer, D. D. (2000) *Neuroscience* **95,** 603–616
75. Hauser, K. F., McLaughlin, P. J., and Zagon, I. S. (1987) *Brain Res.* **416,** 157–161
76. Hauser, K. F., Houdi, A. A., Turbek, C. S., Elde, R. P., and Maxson, W., 3rd (2000) *Eur. J. Neurosci.* **12,** 1281–1293
77. Liao, D., Lin, H., Law, P. Y., and Loh, H. H. (2005) *Proc. Natl. Acad. Sci. U.S.A.* **102,** 1725–1730
78. Narita, M., Kuzumaki, N., Miyatake, M., Sato, F., Wachi, H., Seyama, Y., and Suzuki, T. (2006) *J. Neurochem.* **97,** 1494–1505
79. Rios, C., Gomes, I., and Devi, L. A. (2006) *Br. J. Pharmacol.* **148,** 387–395
80. Liao, D., Grigoriants, O. O., Loh, H. H., and Law, P. Y. (2007) *J. Neurophysiol.* **97,** 1485–1494
81. Liao, D., Grigoriants, O. O., Wang, W., Wiens, K., Loh, H. H., and Law, P. Y. (2007) *Mol. Cell. Neurosci.* **35,** 456–469
82. Lin, H., Higgins, P., Loh, H. H., Law, P. Y., and Liao, D. (2009) *Neuropsychopharmacology* **34,** 2097–2111
83. Liska, D. J., Hawkins, R., Wikstrom, K., and Bornstein, P. (1994) *J. Cell. Physiol.* **158,** 495–505
84. Miljkovic-Licina, M., Gauchat, D., and Galliot, B. (2004) *Biosystems* **76,** 75–87
85. Kauer, J. A., and Malenka, R. C. (2007) *Nat. Rev. Neurosci.* **8,** 844–858
86. Ueda, H., and Ueda, M. (2009) *Front. Biosci.* **14,** 5260–5272
87. Allen, N. J., and Barres, B. A. (2005) *Curr. Opin. Neurobiol.* **15,** 542–548